

Article

Study the Effect of Etching Current Time on Porous Silicon Preparation

Semaa Jamal Saud^{1*}, Donia Ahmed Shaker², Teeba Qais Hammed³, Haitham T. Hussein⁴

1,2,3,4 University of Technology, Department of Applied Science, Iraq

* Correspondence: semaajamal68@gmail.com

Abstract: This study aims to investigate the effect of etching current time on the preparation of porous silicon using the photoelectrochemical etching method. N-type silicon (111) with a resistivity of 1.5-4 Ω .cm was used to prepare the porous silicon layers. The etching process was carried out using a solution of hydrofluoric acid (HF) with a concentration of 18% mixed with high-purity ethanol. The etching current densities were varied at 10, 15, 20, and 30 mA/cm² with an etching time of 15 minutes. The structural and morphological characterization of the porous silicon layers was performed using X-ray diffraction (XRD), Scanning Electron Microscopy (SEM), and Atomic Force Microscopy (AFM). The XRD results showed a broad diffraction peak as the crystal size decreased to the nanometer scale. SEM and AFM images revealed that the porous silicon layer had a sponge-like structure, with pore sizes increasing as the etching current density increased.

Keywords: Porous Silicon, Photoelectrochemical Etching, Etching Current Density, XRD Characterization, Nanopore Morphology

1. Introduction

Semiconductor materials, such as silicon, have electrical characteristics that fall between insulators and conductors. Semiconductors have an almost empty conduction band and a fairly full valence band, as well as an extremely wide energy gap of 3.0eV. There are two types of semiconductors:

- a. Intrinsic Semiconductors
- b. Extrinsic Semiconductors

Intrinsic Semiconductor is one form of semiconductor material in its purest form, with enough energy for electrons to pass crossing the narrow energy gap from the valence band to the conduction band. The number of electrons in Intrinsic Semiconductors equals the number of gaps holes [1].

Extrinsic semiconductors are formed when an intrinsic semiconductor is disturbed by very tiny amounts of impurities or doping (almost 1 part in 10⁸). Extrinsic semiconductors are classified as n-type or p-type based on the kind of doping substance [2]. Semiconductor nanostructures have gained popularity due to their physical characteristics and several applications that are not accessible in bulk semiconductors. Semiconductor nanostructures with a Bohr exciton radius (aB) of 2- 50nm or less, as defined by eq. (1.1).

Citation: Semaa Jamal Saud. Study the Effect of Etching Current Time on Porous Silicon Preparation. Central Asian Journal of Theoretical and Applied Science 2024, 5(4), 445-454

Received: 10th July 2024

Revised: 13th July 2024

Accepted: 24th July 2024

Published: 31st July 2024



Copyright: © 2024 by the authors. Submitted for open access publication under the terms and conditions of the Creative Commons Attribution (CC BY) license (<https://creativecommons.org/licenses/by/4.0/>)

$$\alpha_B = \frac{\epsilon_0 \epsilon_r h^2}{\pi m e^2} \quad (2.1)$$

Where, (ϵ_0) permittivity in the free space, (ϵ_r) relative permittivity, (m^*) reduced mass, (h) Planck's constant, and (e) electron charge [2-4]

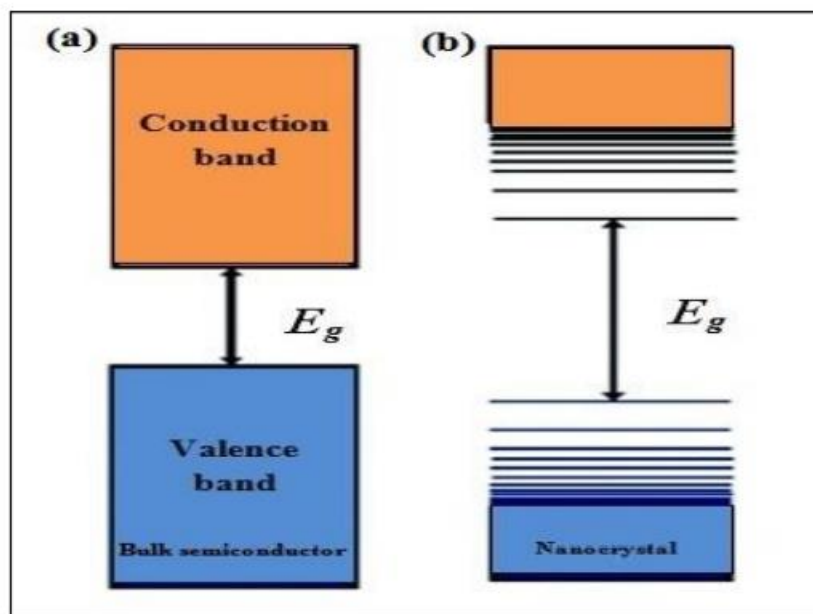


Fig. (1.1) Diagram of the electronic structure of (a) Bulk semiconductor and (b) nanostructure [5].

Semiconductors nanoparticles may be manufactured in a number of forms, including 0D (cubes, pyramids, stars, spheres, and other polyhedral), 1D (zig-zag wires or straight and nanorods), and 2D (disks and platelets) [3].

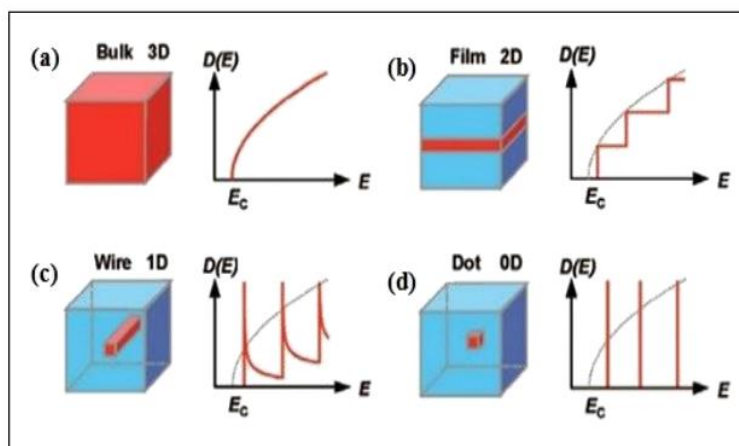


Figure (1.2) A simplified illustration of state density in semiconductors in 3D, 2D, 1D, and 0D. [6].

Silicon Nanostructures

In the high-density electronic industry, silicon is one of the most essential elements. Nanocrystalline silicon is a good approach to turn silicon into a photonic material because the tiny scale causes novel quantum processes that yield some extra special benefits [7].

Quantum effects caused by the retention of electrons and holes in matter cause material characteristics to vary dramatically in nanometers. Furthermore, like the van der Waal forces, etc... [7]. at ambient temperature, crystalline silicon (c-Si) has a tiny energy gap

of approximately 1.12eV, making it a non-emitter of visible light (10^{-6} - 10^{-7}) and extremely pure with bonding energy of about 14MeV. The threeparticle process of radioactive recombination of excited electrons in the conduction band and holes in the valence band involves a momentum-conserving phonon [8].

The nanoscale causes a new quantum phenomenon, which produces several extraordinary benefits. Material properties vary dramatically at the nanoscale due to quantum phenomena caused by hole and electron confinement in the material. Furthermore, at the nanoscale, weak range forces such as Vander Waal forces dominate. When the semiconductor nanostructure size approaches a radius of exciton Bohr, "dimensions represent the excitons specific of (e-h) pairs in the semiconductor at the range around (2 to 50) nm depending on the material type." The effect of quantum confinement will begin, changing the electrical and optical properties, For example, when the nanostructure size decreases, the energy gap (E_g) increases, as seen in figure (1.1) [1-3], where the bands of energy are separated into distinct levels and the bandgap is transformed from indirect to quasi-direct.

Classification of PS

The Stands for Pore Size Classification, which may range from a few nanometers to a few microns depending on the formation variables [9]. The wide classification of PS elements, as indicated in Table, determines the regimes (1.1)

Table (1.1) PS material classification.

	Width of the dominant pore	Kind of material
1.	Less than 2 nm	Micro-porous
2.	Between the range 2 nm to 50 nm	Meso-porous
3.	Greater than 50 nm	Macro-porous

Pores are called micro or nano when their diameter and spacing are equal to or less than 2 nm. As shown in figure (1.3a) [10], it has a sponge-like structure and is extremely efficient for light emission. Mesopores are defined as pores with a diameter of 2 to 50 nanometers. In Si, the creation of these pores is inefficient in terms of light emission, as seen in image (1.3b).

Macropores are holes in silicon that are larger than 50 nanometers in diameter. In terms of light emission efficiency, it is similar to mesopores. Nonetheless, the structure of these pores is intriguing. It has the smooth pore walls and have very specific pore development directions, as seen in figure (1.3c) [11].

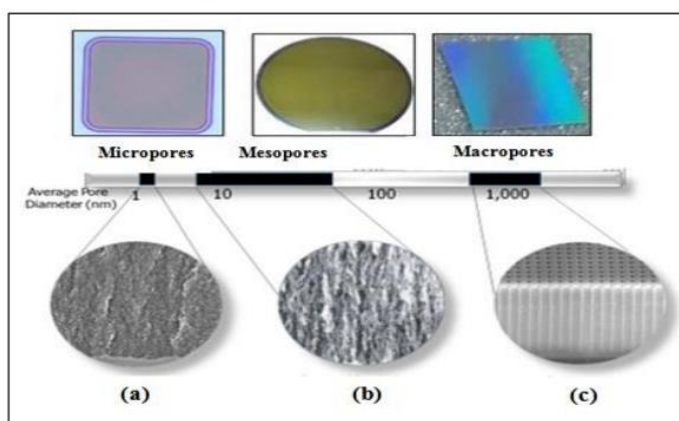


Figure (1.3) depicts three types of pores: (a) micropores, (b) mesopores, and (c) macropores [1].

The fundamentals

of the porous silicon production process One of the benefits of porous silicon is how easy it is to prepare. The basic mechanisms of PS formation are as follows:

1. Etching by the photochemical method.
2. Etching by the photo-electrochemical etching method.
3. Etching by stain method.
4. Etching by electrochemical method.

Porous silicon photo-electrochemical etching

Photoelectrochemical etching (PECE) is the technology used in my project, which is outlined below:

Because the etching of n-type or p-type silicon into HF solution is feasible, this method is regarded as a critical technology in businesses that prefer PS architectures. This is owing to the fact that the PECE approach combines two types of etching procedures (electrochemical and photochemical).

Thonissen and Juhasz [12,13]. PS has been referred to as both n-type and p-type lighting. There are huge differences in the shapes of the strata at one time throughout the development. 37 The supply holes in the layer over the semiconductor regulates anodic dissolution. On the surface of n-type silicon, bit holes will be present. The illumination of the semiconductor/electrolyte interface can increase the density of holes at the silicon. The n-type PS visible under PECE illumination is composed of nanoporous silicon layers that shield a macroporous silicon layer with pores measured in microns [14].

To perform anodization etching, the semiconductor is submerged in conductive electrolyte using a Teflon cell that is resistant to HF in the PECE process. The silicon is biased as the anode, while the cathode is a platinum or HF resistant conductive material, with the silicon sample submerged in an electrolyte solution containing various amounts of HF, ethanol, or methanol. The PECE method's experimental setup is depicted in Figure (1.2).

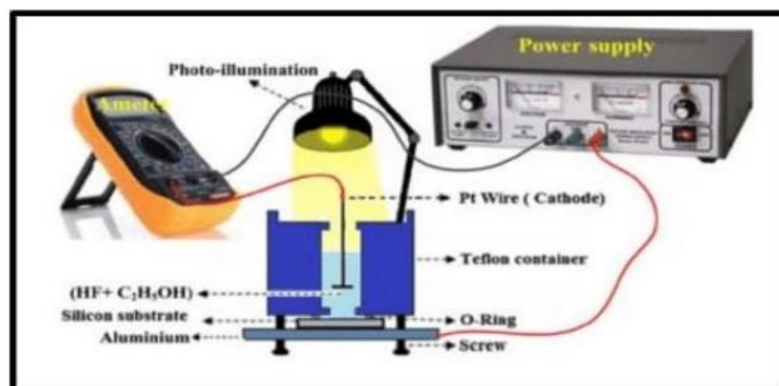


Figure (1.4): Schematic design of a Photoelectrochemical etching system [15].

Porous silicon applications

Porous silicon is a semiconductor substance that has a wide range of uses [2]. Table (1.2) summarizes the probable applications of porous silicon, and shows utility for every application Porous silicon was employed in this investigation as a sensing application for gas detection; many broad applications will be explained in detail in the following subsections.

Table (1.2): potential applications area of PS [3]

Application area	Role of porous silicon	Key property
Optoelectronics	LED Waveguide Field emitter Optical memory	Efficient electroluminescence Tenability of refractive index Hot carrier emission Non-linear properties
Micro-optics	Fabry-Perot Filters Photonic bandgap structures All-optical switching	Refractive index modulation Regular macrospore array Highly non-linear properties
Energy conversion	Antireflection coatings Photo-electrochemical cells	Low refractive index Photo corrosion cells
Environmental monitoring	Gas sensing	Ambient sensitive properties
Microelectronics	Micro-capacitor Insulator layer Low-k material	High specific surface area High resistance Electrical properties
Wafer technology	Buffer layer in heteroepitaxy SOI wafers	Variable lattice parameter High etching selectivity
Micromachining	Thick sacrificial layer	Highly controllable etching
Biotechnology	Tissue bonding Biosensor	Tunable chemical reactivity Enzyme immobilization

2. Materials and Methods

Experimental Work

In this chapter deal with the method of preparing porous silicon by a photochemical etching technique. Figure (2.1) shows the scheme of all the experimental used in this work.

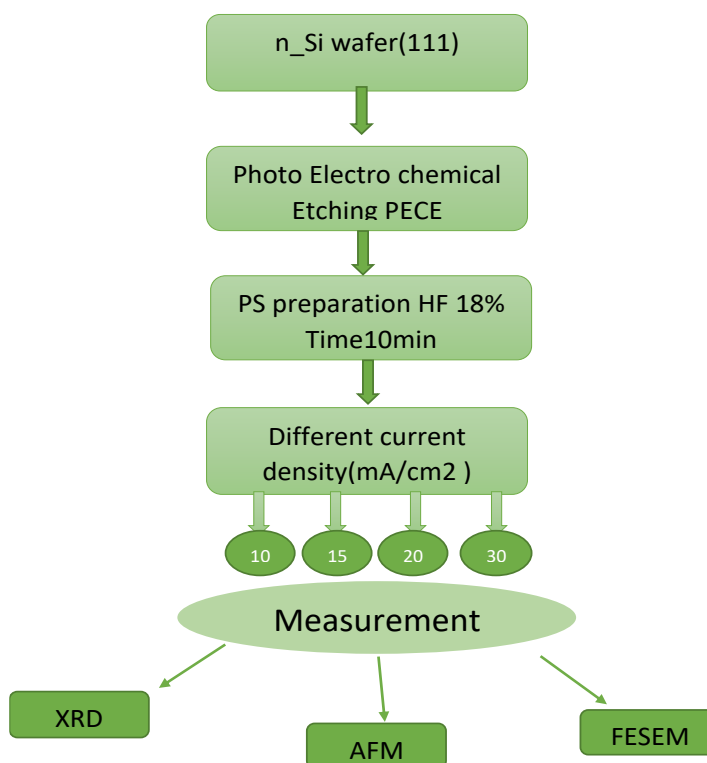


Figure (2.1a) the diagram of the experimental work

Chemicals

Different chemicals were used in the present study as listed in Table (2.3).

Carbon nanotube	Cheaptubes.com	Grafton	USA
Ethanol		Scharlau	Spain
Hydrofluoric acid		Scharlau	Spain

Preparation of Porous Silicon (PS).

The PS layers in this work were prepared using n-type (111) oriented silicon wafer with a thickness of $580 \pm 0.25 \mu\text{m}$ and a resistivity of about ($1.5\text{-}4 \Omega\cdot\text{cm}$.) before etching, we started by dividing the silicon wafer with dimensions of $2.5 \times 2.5 \text{ cm}$. was used to prepare PS surface photo-electrochemical etching (PECE). the Si wafers were cleaned to eliminate any surface contaminants. The cleaning procedure began with eliminating dust particles from the surface by washing them with ethanol alcohol in an ultrasonic bath. The oxides were then removed by rinsing with 18% hydrofluoric acid (HF) for 15 min.

Photo Electro-chemical etching process (PECE).

The PS layer has been prepared by using the PECE process, the system of this process consists of D.C power supply as a source of the current, Ammeter to measure the current density, n-type silicon wafer used as an anode electrode, mesh of gold as cathode electrode, and the etching solution consists Hydrofluoric acid (HF) 18%, and it was diluted with high purity ethanol solution $\text{C}_2\text{H}_5\text{OH}$ 99.8%, to prepare concentration of about 18% HF. In this technique, the HF container is made of Teflon duo to its high resistance for HF and to prevent any chemical interaction Carbon nanotube Cheaptubes.com Grafton USA Zinc Sigma-Aldrich USA Oxalate Sigma-Aldrich USA Ethanol Scharlu Spain Hydrofluoric acid Scharlau Spain Methanol Scharlau Spain Acetone Sigma-Aldrich USA Field emission scanning electron microscopy Mira 3-XMU Czech 65 with HF.

The rubber O-ring is utilized before the top portion of the cell. The latest has a central circular of (1.2 cm) to let touching the silicon layer. The two electrodes applied current onto the cell. The lower one is stainless steel foil below the silicon layer and the upper is gold mesh attached with the HF solution The Si wafers were divided into small pieces with dimensions about of $2.5 \text{ cm} \times 2,5\text{cm}$ and rinsed in ethanol $\text{C}_2\text{H}_5\text{OH}$ for 15min with ultrasonic to clean and remove any contamination on the surface. The samples were prepared in different current density $J=10, 15, 20$ and, 30 mA/cm^2 , HFC of concentration 15%, and time of etching 15 min. The adding of ethanol solution into the etching electrolyte is playing the main role to reducing the tension of the surface and improving the uniformity and homogeneity of the PS layers by enhanced removal of hydrogen bubbles after the process of etching. The HF consecration were prepared with 40% by using the equation.

$$C_1V_1 = C_2V_2 \dots\dots\dots (3.1)$$

Where C_1 concentration of HF before diluted, V_1 volume of HF only, C_2 The concentration of HF after diluted, V_2 volume of HF, and ethanol solution. After the etching process complete will be using air drier. Figure (3.2) shows the schematic and photograph image of PECE set up.

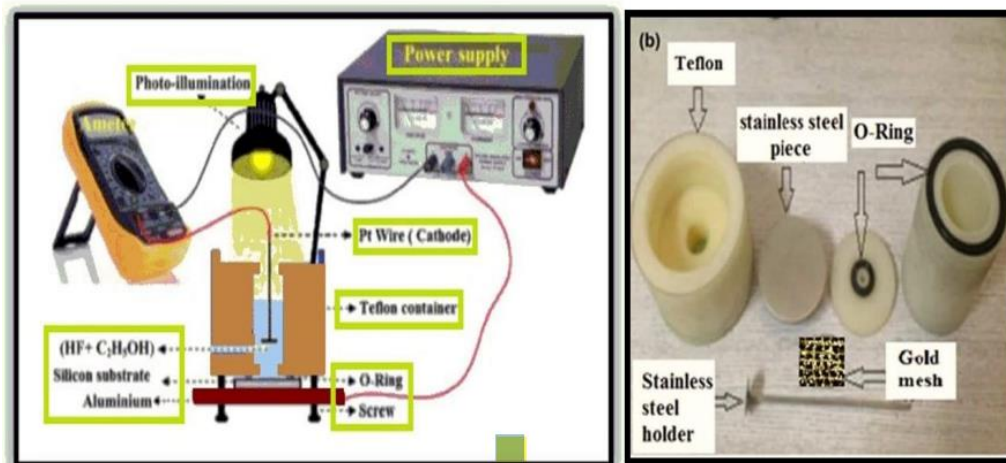


Figure (2.2): shown (a) schematic of PECE cell (b) Photograph image of PECE set up.

Measurements

Many measurements have been conducted in this work such as:

Scanning Electron Microscope

(SEM) SEM instrument type inspects 50 used to analyze and describe the morphology of surface for all samples: PS. SEM test is necessary for investigating the nanometric scale by imagining the surface. SEM test was conducted in the Applied Science Department /University of Technology/ Iraq.

XRD

XRD system is one important test for investigating the structural properties of a specimen, which tracks the intensity as a function of Bragg's angles. Both samples in this work have been subjected to this examination.

Atomic Force Microscopy (AFM)

The morphological properties of the PS with different etching density (10,15, and 30 mA/cm² samples were studied by Atomic Force Microscopy (AFM), (SPM AA3000).

Angstrom Advanced Inc., USA AFM contact mode); AFM instrument was achieved in the department of Chemical Science- Baghdad University.

3. Results and Discussion

This chapter contains the results, examination and discussions of experimental measurements for samples of porous silicon prepared by photo electrochemical etching technique (PECE). The structural, optical, chemical, and surface characteristics were investigated for PS samples using XRD, FESEM and AFM methods.

Structure Properties of Porous Silicon

Crystalline silicon with nanoscale crystals leads to make up the PS material. X-ray crystallographic shown that PS's skeleton retains the structure of a single crystal after anodization, which is significant. The XRD diffraction analysis was carried out to investigate the structural characteristics of PSi samples. The XRD patterns have been illustrated in Figure (4.1) which shows peaks of silicon crystal and porous silicon layer prepare at current etching density $J=10,20$ and 30mA/cm^2 , time etching 15 min, and $\text{HFc}=18\%$. These results showed that PSi layers are still crystallized in the plane [46], but the PSi layer is slightly shifted to the small (2θ) $=28.48^\circ, 28.4^\circ$, and 28.42° for, PSi at $J=10,20$ and 30mA/cm^2 respectively. A little increase in lattice parameter leads to a modest shift in the PSi peak diffraction angle due to the strain effect. A smaller nanocrystalline domain

results in a wider diffraction peak, which becomes wider as crystal size decreases to the nanometric scale [17].

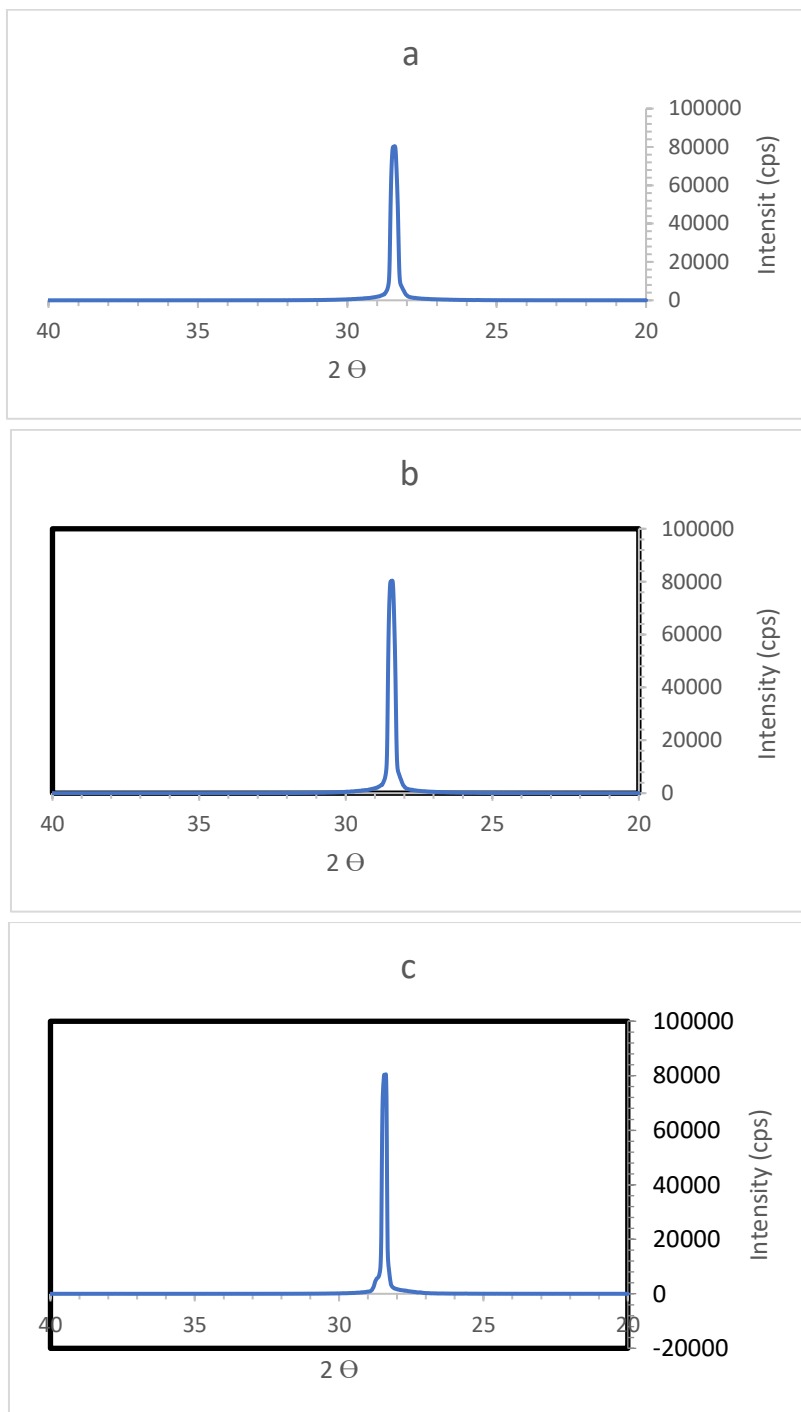


Figure (3.1) shows XRD diffraction peaks of a) PSi at $J=10$, b) 20 and c) 30 mA / cm² , HFC of 18%, and time etching of 15minutes.

4. Conclusion

The article investigates the impact of etching current density on the preparation of porous silicon (PS) using a photoelectrochemical etching (PECE) technique. The study utilized n-type silicon wafers and varied etching current densities (10, 15, 20, and 30 mA/cm²) with a constant etching time of 15 minutes. The structural and morphological properties of the PS layers were analyzed using X-ray diffraction (XRD), Scanning Electron Microscopy (SEM), and Atomic Force Microscopy (AFM).

Key findings include:

- a. XRD Results: The PS layers retained a crystalline structure, but the crystal size decreased to the nanometer scale, leading to a broadening of the XRD diffraction peaks.
- b. SEM and AFM Analysis: The PS layers displayed a sponge-like structure, with pore sizes increasing as the etching current density increased. The PS layers exhibited nanometer-scale pores, which have potential applications in various fields such as gas sensing and optoelectronics.

The study concludes that the etching current density significantly influences the structural and morphological characteristics of PS, which can be tailored for specific applications.

REFERENCES

1. Akinyele, Daniel, Elijah Olabode, and Abraham Amole. "Review of fuel cell technologies and applications for sustainable microgrid systems." *Inventions* 5, no. 3 (2020): 42.
2. Bisi, O., Ossicini, S., & Pavesi, L. (2000). "Porous silicon: A quantum sponge structure for silicon based optoelectronics." *Surface Science Reports*, 38(1-3), 1-126.
3. Bisi, Olmes, Stefano Ossicini, and Lorenzo Pavesi. "Porous silicon: a quantum sponge structure for silicon based optoelectronics." *Surface science reports* 38, no. 1-3 (2000): 1- 126.
4. Canham, L. T. (1990). "Silicon quantum wire array fabrication by electrochemical and chemical dissolution of wafers." *Applied Physics Letters*, 57(10), 1046-1048.
5. Chang, Jin, and Eric R. Waclawik. "Colloidal semiconductor nanocrystals: controlled synthesis and surface chemistry in organic media." *RSC Advances* 4, no. 45 (2014): 23505-23527.
6. Chen, Tupei, and Yang Liu. *Semiconductor Nanocrystals and Metal Nanoparticles: Physical Properties and Device Applications*. CRC Press, 2016.
7. Collins, Reuben T., and Philippe M. Fauchet. "Porous silicon: From luminescence to LEDs." *Physics Today* 50, no. 1 (1997): 24-31.
8. Cullis, A. G., Canham, L. T., & Calcott, P. D. J. (1997). "The structural and luminescence properties of porous silicon." *Journal of Applied Physics*, 82(3), 909-965.
9. de Mello Donegá, Celso, ed. *Nanoparticles: workhorses of nanoscience*. Springer, 2014.
10. Dwivedi, Priyanka, Saakshi Dhanekar, and Samaresh Das. "Selective acetone electrical detection using functionalized nano-porous silicon." In *2015 Annual IEEE India Conference (INDICON)*, pp. 1-4. IEEE, 2015.
11. Kassa T. T. ,*SiliconNanostrucres,M.ScThesis, Addis Ababa University, Ethiopia (2006)*.
12. Kumeria, T., & Santos, A. (2018). "Porous silicon for therapeutic applications: Recent advances and future perspectives." *Expert Opinion on Drug Delivery*, 15(5), 487-499.
13. Liu, Yucheng, Yunxia Zhang, Xuejie Zhu, Zhou Yang, Weijun Ke, Jiangshan Feng, Xiaodong Ren et al. "Inch-sized high-quality perovskite single crystals by suppressing phase segregation for light-powered integrated circuits." *Science Advances* 7, no. 7 (2021): eabc8844.
14. McAllisterMJ, LiJL, and H. AdamsonD. "Singlesheetfunctionalizedgraphenebyoxidationandthermalexpansionofgraphite." *Chem Mater* 19 (2007): 4396-4404.
15. Mohammed, Ameer Hussein, and H. A. R. Akkar. "Design and Implementation of Artificial Neural Network for Mobile Robot based on FPGA." *University of Technology (2015)*.
16. Padidar, M., A. Jalalian, M. Abdouss, P. Najafi, N. Honarjoo, and J. Fallahzade. "Effets of nanoclay on some physical properties of sandy soil and wind erosion." *International Journal of Soil Science* 11, no. 1 (2016): 9-13.
17. Prabhu, R. R., & Seshadri, M. (2010). "Porous silicon as a biomaterial for applications in drug delivery, tissue engineering and biosensing: A review." *Sensors and Actuators B: Chemical*, 155(1), 155-168.

18. Praveenkumar, S., D. Lingaraja, P. Mahiz Mathi, and G. Dinesh Ram. "An experimental study of optoelectronic properties of porous silicon for solar cell application." *Optik* 178 (2019): 216-223.
19. Sahu SN, Nada KK. *NanoStructure Semiconductors: Physics and Applications*. Institute of Physics in India.;Vol.67(1):PP.103-130 (2001).
20. Sailor, M. J., & Link, J. R. (2005). "Smart dust: Nanostructured devices in a grain of sand." *Chemical Communications*, 11, 1375-1383.
21. Salonen, J., & Lehto, V. P. (2008). "Fabrication and chemical surface modification of mesoporous silicon for biomedical applications." *Chemical Engineering Journal*, 137(1), 162-172.
22. Shabir, Qurrat, A. Pokale, Armando Loni, D. R. Johnson, L. T. Canham, Roberto Fenollosa, M. Tymczenko et al. "Medically biodegradable hydrogenated amorphous silicon microspheres." *Silicon* 3, no. 4 (2011): 173-176.
23. Sun, Wentong, Yu Han, Zhenhua Li, Kun Ge, and Jinchao Zhang. "Bone-targeted mesoporous silica nanocarrier anchored by zoledronate for cancer bone metastasis." *Langmuir* 32, no. 36 (2016): 9237-9244.
24. Torres-Costa, V., & Martín-Palma, R. J. (2010). "Applications of porous silicon in optoelectronics, microelectronics, and energy technologies." *Materials*, 3(4), 3052-3085.
25. Wang, P. C., & Ni, S. B. (2015). "Recent advances in porous silicon–metal oxide nanocomposites: Synthesis and applications in energy storage." *Journal of Power Sources*, 282, 230-239.
26. Zhao, J., & Song, K. (2016). "Advances in porous silicon research for biomedical applications." *Journal of Biomedical Nanotechnology*, 12(1), 1-16.